Fracture-generated permeability and groundwater yield in Norway

AGUST GUDMUNDSSON, INGRID FJELDSKAAR & OTILIE GJESDAL

Gudmundsson, A., Fjeldskaar, I. & Gjesdal, O. 2002: Fracture-generated permeability and groundwater yield in Norway. *Norges geologiske undersøkelse Bulletin 439*, 61–69.

The transport of groundwater in bedrock is largely determined by interconnected fractures and their apertures. The conditions by which fractures become interconnected are thus of primary importance in understanding permeability and groundwater yield. This applies in particular to the observed linear correlation between the current postglacial uplift rate and groundwater yield in the bedrock of southern Norway. We present boundary-element models on the formation of interconnected fracture pathways with application to the coastal areas of West Norway. In the models, we use external tensile stress and internal fluid overpressure; loading conditions that are likely to have been operative in large parts of Norway during the Holocene. The external tensile stress results indicate that many fracture pathways form by the linking up of offset joints through transverse shear fractures. Other pathways, however, are formed by linking up of joints and contacts through tensile stresses associated with the tips of propagating hydrofractures. How the fracture pathways form may affect the subsequent permeability. In particular, transverse shear fractures are likely to have relatively small apertures and limit the groundwater transport.

Agust Gudmundsson, Ingrid Fjeldskaar & Otilie Gjesdal. Geological Institute, University of Bergen, Allegaten 41, N-5007 Bergen, Norway (e-mail: agust.gudmundsson@geol. uib.no)

Introduction

The observed linear and positive correlation between the current rate of postglacial uplift and yield of groundwater wells is one of the basic hydrogeological relations in Norway. This correlation was initially published by Rohr-Torp (1994), using five areas of different postglacial uplift rates and including a total of 1278 drilled wells in the bedrock of southern Norway. His results were supported by those of Morland (1997) who used a database of 12,757 bedrock wells, of which 8,726 are in Precambrian rocks.

This correlation may be related to increase in hydraulic conductivity in areas of high uplift rates compared with those of low uplift rates (Gudmundsson 1999). High uplift rates would then coincide with areas of crustal doming where associated tensile stresses lead to reactivation of old, or formation of new, water-conducting fractures. However, a fracture system conducts water only if the percolation threshold of that system is reached, that is, only if the fractures form an interconnected cluster (Stauffer & Aharony 1994). Thus, in order to understand how uplift-generated stress fields contribute to groundwater yield, we must also understand how fractures link up into interconnected, water-conducting systems.

This paper has three principal aims. First, to present field examples of evolving small-scale fracture systems as an indication of permeability development. All the examples are from the island of Øygarden just west of the city of Bergen. Second, to present numerical models on how fracture systems link up in jointed and layered rock masses. The focus is on the propagation of the two main types of fractures:

extension fractures, which include many joints and tension fractures, and shear fractures, i.e., faults. Third, to discuss the postglacial stress fields in Norway in relation to the linking up of fractures.

Fracture systems and faults

In many rocks, groundwater flow is primarily through fracture systems, some of which eventually develop into large-scale faults. The fracture networks may be primary structures such as, for example, many joint systems in sedimentary and igneous rocks. Commonly, these primary fractures form weaknesses from which interconnected tectonic fracture systems and faults develop.

As an example of a largely unconnected fracture system, one may consider exfoliation fractures (sheet joints) in layered gneiss on the island of Øygarden (Fig. 1). These fractures, subparallel with the free surface, form as a result of rapid unloading of the surface due to erosion and deglaciation. Removal of the overburden leads to the surface-parallel compressive stresses exceeding the vertical stress. The result is fracture development parallel to the maximum compressive stress and, therefore, parallel with the surface. The horizontal exfoliation fractures give rise to mechanical layering which partly follows the original layering in the gneiss, but is partly independent of that layering (Fig. 1). Thus, the rock becomes divided into sheets which, however, decrease rapidly in frequency with depth (Fig. 1, cf. Johnson 1970).

Exfoliation fractures that become interconnected may contribute to bedrock permeability at shallow depths. They, like other fractures, become interconnected through either

Fig. 1. Suhorizontal exfoliation fractures in gneiss on the island of Øygarden (Toftøy), West Norway. Spacing of the exfoliation fractures increases rapidly with depth. View northeast; the subvertical normal fault west of the person is the one in Fig. 3.

extension fractures or shear fractures. In an extension fracture the displacement is primarily perpendicular to, and away from, the fracture plane (Fig. 2), whereas in a shear fracture the main displacement is parallel with the fracture plane (Fig. 3).

Fig. 2. Linking up of extension fractures in gneiss on the island of Øygarden (Toftøy). View northeast; the fracture aperture tends to increase when meeting with the horizontal exfoliation fractures, at the contacts with the dark amphibolite layers. The steel tape is 1 m long.
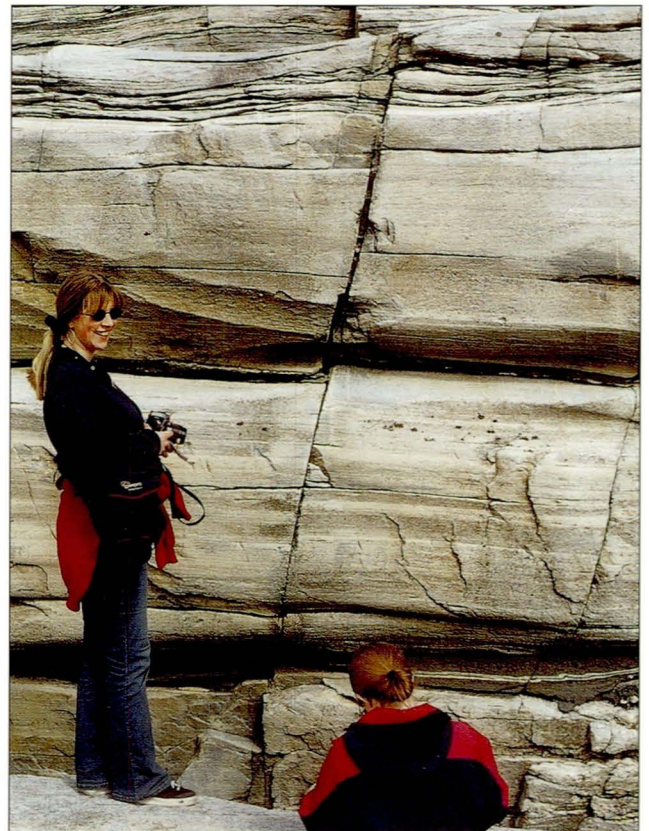

Fig. 3. Steeply dipping normal fault interconnecting subhorizontal exfoliation fractures in the gneiss of Øygarden (Toftøy) (Fig. 1). Maximum vertical displacement is 4 cm in the centre of the fault, but decreases to zero at the tips. View northeast; the persons provide a scale.

Extension fractures

Extension fractures (Fig. 2) are either tension fractures or hydrofractures. Tension fractures form when the minimum principal compressive stress (considered positive) is negative, that is, when there is an absolute tension in the crust.
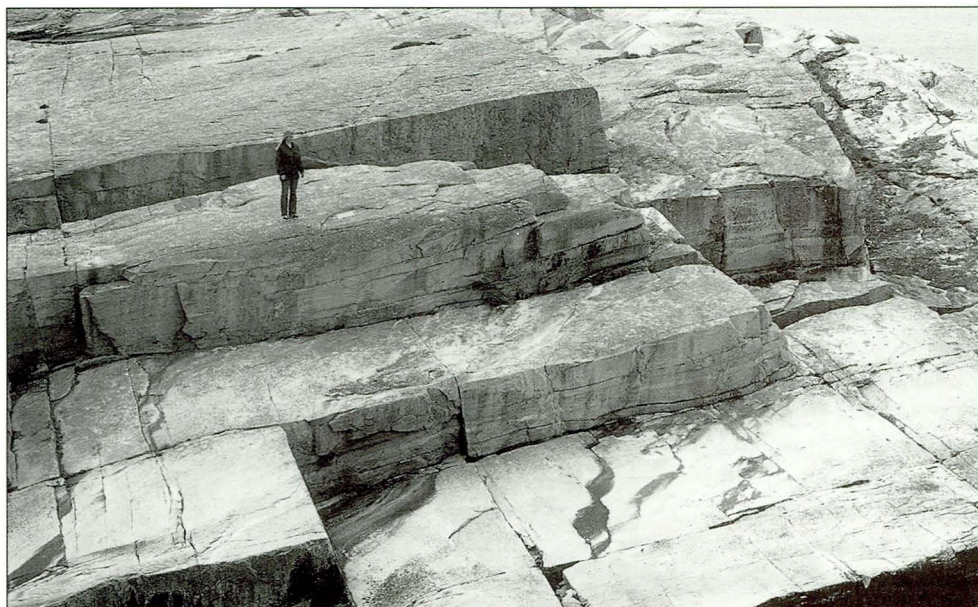
Fig. 4. Well interconnected, orthogonal joint system in gneiss on the island of Øygarden (Toftøy). View southwest; the person provides a scale.

They are mostly limited to areas undergoing active extension, such as areas of rifting and those of great postglacial uplift such as in the central part of Fennoscandia (Mörner 1980, Gudmundsson 1999). The maximum depth to which a tension fracture can propagate d_{max} from the surface (before it changes into a normal fault) is given by (Gudmundsson 1992, 1999):

$$d_{max} = \frac{3T_0}{\rho_r g} \qquad (1)$$

where T_0 is the in situ tensile strength, ρ_r the density of the host rock, and g the acceleration due to gravity. The joints in Figs. 2 and 4 are in a crustal layer with an average density of around 2500 kg m^{-3} (Hansen 1998). If these joints are tension fractures, their maximum depths can be estimated from Eq. (1). Typical in situ strengths of bedrock are 0.5-6 MPa (Amadei & Stephansson 1997), and the acceleration due to gravity at the surface is $g = 9.8$ m s^{-2}. Substituting these values in Eq. (1), we obtain d_{max} as around 60 m (for $T_0 = 0.5$ MPa) and 700 m (for $T_0 = 6$ MPa).

The presumed tension joints in Figs. 2 and 4 are unlikely to reach the above maximum depth because the horizontal exfoliation fractures would tend to arrest the joint tips. Also, there is a correlation between opening of a tension fracture at the surface and its controlling dimension, defined as the smaller of the fracture dip and strike dimensions (Gudmundsson 2000). For a mechanically layered host rock, the controlling dimension of a fracture is normally its dip dimension (Gudmundsson 1992, 2000). Thus, tension fractures with maximum surface openings of a few millimetres normally have dip (controlling) dimensions of several metres or, at most, a few tens of metres. The interconnected joint system in Fig. 4 is therefore likely to be limited to the uppermost tens of metres or, at most, a few hundred metres, both as regards the depth of the exfoliation fractures as well as the depth of the vertical tension joints.

In contrast to tension fractures, hydrofractures can occur at any crustal depth. Hydrofractures are opened up by a fluid pressure that is greater than the normal stress on the fracture plane. Most hydrofractures are extension fractures (Gudmundsson et al. 2001), in which case the normal stress on the hydrofracture plane is the minimum principal com-
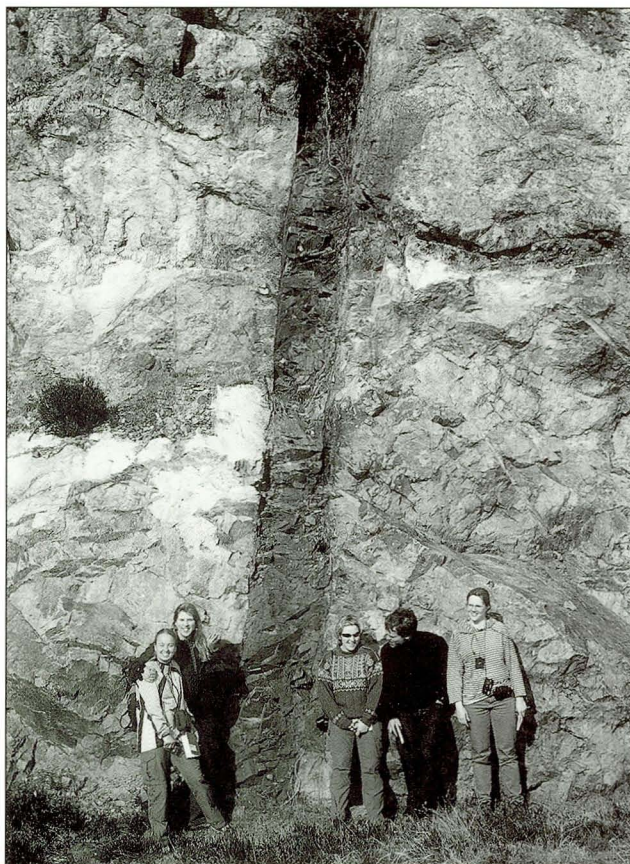

Fig. 5. Dolerite dyke, of Permian age, on the island of Tysnesøy, south of Bergen, West Norway. View northeast; the dyke is 0.7 m thick and dips 77°NW.

pressive stress. The normal condition for hydrofracture formation can thus be given as (Jaeger & Cook 1979):

$$P_t \approx \sigma_3 + T_0 \qquad\qquad (2)$$

where P_t is the total fluid pressure, σ_3 is the minimum compressive principal stress (normal to the hydrofracture), and T_0 is the in situ tensile strength of the host rock.

Because hydrofractures can form at any crustal depth, they are likely to be generally more important for the development of fracture pathways and permeability in rocks than tension fractures. For example, many joints (Figs. 2, 4) may form as hydrofractures where the fluid disappears subsequent to the joint formation. In general, where groundwater or gas is the fluid that drives a fracture open, it is difficult to confirm that the fracture was generated by a fluid. Other fractures, however, are generated by fluids or magma that freeze in the fracture subsequent to its formation. Well known examples are dykes, sills, inclined sheets and mineral-filled veins. Commonly, mineral veins form networks of extinct geothermal systems that provide important information on permeability generation through their emplacement (Gudmundsson et al. 2001). Some veins may reach lengths of several hundred metres, but most have lengths of several metres or less (Gudmundsson et al. 2001), and are thus individually too small to have much effect on groundwater flow.

Thick sills can have considerable effects on groundwater flow, but generally the most important 'frozen' hydrofractures for groundwater flow are regional dykes (Fig. 5). In Norway, dykes are common along the west coast and in the Oslo region (Thon 1985, Sundvoll & Larsen 1993, Torsvik et al. 1997, Fossen & Dunlap 1999). Many dykes are of dense basalt or dolerite with low matrix permeability and act as barriers to transverse flow of groundwater. Others, particularly thick and fractured dykes, may be sources of groundwater (Singhal & Gupta 1999).

Perhaps the most important effect of dykes on groundwater flow in Norway, however, is that the basaltic dyke rock has normally very different mechanical properties from its host rock (Fig. 5). It follows that stresses tend to concentrate at the contact between the dyke rock and the host rock and generate fractures that may conduct groundwater. Dykes form their pathways in a similar way to that in the models of hydrofracture formation below. It follows that groundwater conduits at contacts between dyke rock and host rock will follow these same pathways.

Faults

Faults may initiate as small-scale shear fractures (Fig. 3) or, perhaps more commonly, develop during the linking up of small fractures of various types (Fig. 6). In vertical sections, shear fractures (like tension fractures) normally have difficulty in propagating through horizontal discontinuities such as open exfoliation fractures (Fig. 3). At such discontinuities, a shear fracture may either become offset or arrested.

Fig. 6. Extension fractures linked up through transverse shear fractures, modelled in Figs. 7-8. View NNE; the length of the steel tape is 0.8 m.

In lateral sections (Fig. 6), shear fractures (and extension fractures) normally grow by the linking up of gradually larger segments. These segments may initially be offset joints formed early in the evolution of the host rock. Alternatively, later-formed tectonic fractures may propagate and link up into larger, segmented fractures (Fig. 6). In doing so, they form an interconnected system of fractures or segments that has the potential of conducting groundwater along its entire length.

The linking up of small-scale joints and fractures into larger shear fractures or fracture systems is, in detail, a complex process that is still only partly understood (Cox & Scholz 1988, Gudmundsson 1992, Acocella et al. 2000, Mansfield & Cartwright 2001). This process, however, largely controls whether or not the percolation threshold of a fracture system is reached and, thereby, the bedrock permeability. Some general aspects of linking up of fractures into segmented extension fractures and shear fractures are illustrated by the following numerical models.

Numerical models of fracture growth

All the models are made using the boundary-element program BEASY (1991), the method being described in detail by
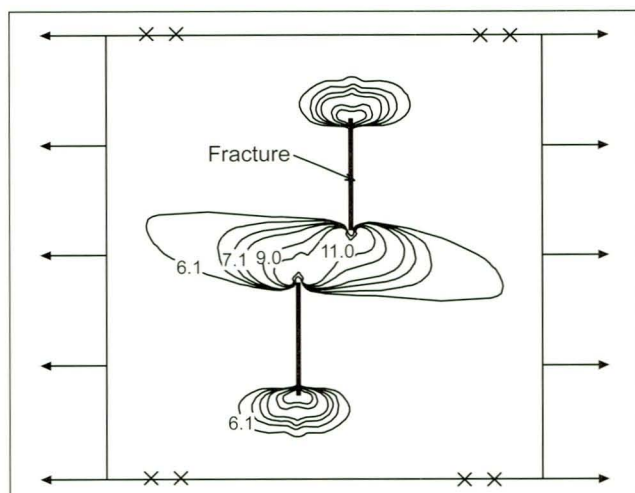
Fig. 7. Boundary-element model showing the tensile stress, in mega-pascals as absolute values, between the nearby tips of two extension fractures of equal length subject to 6 MPa tensile loading (indicated by horizontal arrows). In this model, the offset (horizontal distance) and underlapping (vertical distance) between the nearby tips are both equal to half the fracture length.
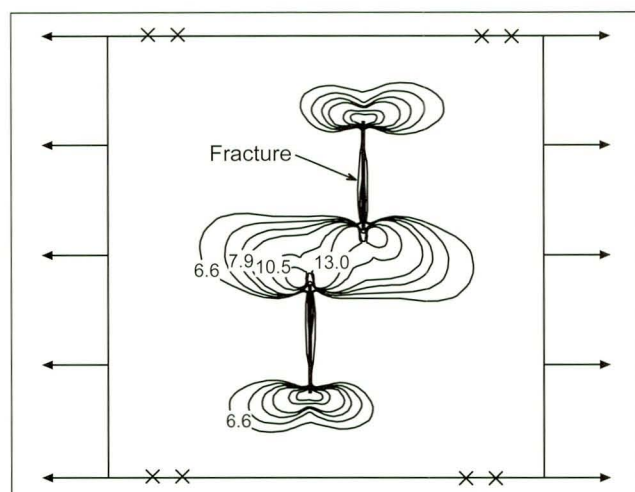

Fig. 8. Boundary-element model showing the shear stress, in mega-pascals, for the same fracture configuration and loading as in Fig. 7.

Brebbia & Dominguez (1989). The program makes it possible, for given boundary conditions, to calculate the stresses and displacements at any points of interest inside the model. The results are most conveniently presented as contours of equal stress magnitude, given in mega-pascals, as well as opening up of discontinuities such as fractures and contacts. The models are divided into one or more zones (corresponding, for example, to mechanical layers), each with uniform mechanical properties; here Young's modulus (also referred to as stiffness) and Poisson's ratio.

The first models (Figs. 7, 8) indicate how offset fractures may link up to form an interconnected system of en echelon segments (Fig. 6). In these models, the only loading on the offset fractures is a fracture-perpendicular tensile stress of 6 MPa, a value similar to the maximum in situ tensile strength

of gneiss (Amadei & Stephansson 1997). This load is applied as tension perpendicular to the two boundaries of the model that run parallel with the fractures (Figs. 7, 8). A uniform Poisson's ratio of 0.25, used in all the models, is appropriate for gneiss (Jumikis 1979, Bell 2000). The uniform Young's modulus used in the first models, 10 GPa, is in the lower range of laboratory values of Young's modulus for gneiss (Jumikis 1979, Bell 2000). Because in situ rocks normally have much lower Young's moduli than small-scale laboratory measurements of the same rock types (Goodman 1989), this value is appropriate. The fractures are modelled as internal springs, each with a stiffness of 6 MPa/m. The units of fracture stiffness differ from those of rock stiffness (Young's modulus) because the stiffness of a solid rock is determined from a stress-strain curve whereas that of a fracture is determined from a stress-displacement curve (Hudson & Harrison 1997).

The results show zones of high tensile (Fig. 7) and shear (Fig. 8) stresses between the nearby tips of the fractures. For the given loading of 6 MPa tensile stress, these zones generate potential tensile stresses in excess of 11 MPa (Fig. 7) and potential shear stresses in excess of 13 MPa (Fig. 8). These are the relevant values, but much higher potential stresses occur at the fracture tips. A tensile stress of 11 MPa is around double the maximum in situ tensile strength of gneiss (Amadei & Stephansson 1997), so that tensile fractures would be expected to form inside the high-stress zone. Similarly, the in situ shear strength of rock, which is commonly roughly twice its tensile strength (Jumikis 1979, Farmer 1983), is also normally much less than 13 MPa, in which case shear fractures would be expected to form in the high-stress zone.

The ESE-WNW-trending and straight transverse fractures connecting the main NNE-SSW-trending fractures in Fig. 6 are likely to be mostly shear fractures. Shear fractures tend to be straight and form inside the zone of maximum shear stress (Fig. 8), whereas most tensile fractures generated in such a high-stress zone are gently curving and form hook-shaped fractures (Gudmundsson et al. 1993, Acocella et al. 2000).

The other models (Figs. 9-12) show how a hydrofracture, driven by an internal fluid overpressure, opens up discontinuities (joints and contacts) in the host rock ahead of the hydrofracture tip. In all these models, the hydrofracture is modelled as a vertical extension (mode I) fracture with an internal fluid overpressure that varies from 10 MPa at the bottom of the fracture to 0 MPa at the fluid front. The fluid front coincides with the fracture tip in the models in Figs. 9-11, but in Fig. 12 the fluid front is 0.1 units below the fracture tip. Each model has a unit height; all the dimensions are given as a fraction of this unit. Only the upper half of each hydrofracture is modelled, and the models are fastened at the lower corners, so as to avoid rigid body translation and rotation.

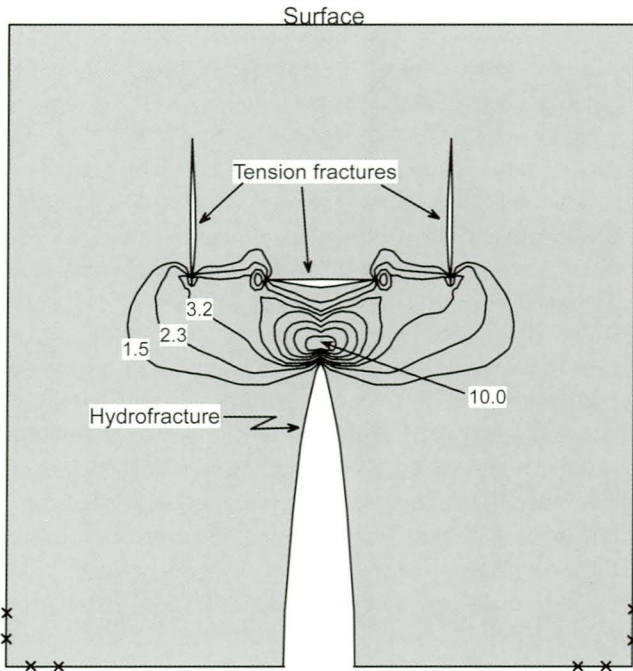As in the earlier models (Figs. 7, 8), a uniform Poisson's

Fig. 9. Boundary-element model showing how the tensile stress, in mega-pascals, around the tip of a vertical hydrofracture opens up vertical joints and a weak contact into tension fractures. Figs. 8-12 show only tensile stresses in the range 1.5-10 MPa.
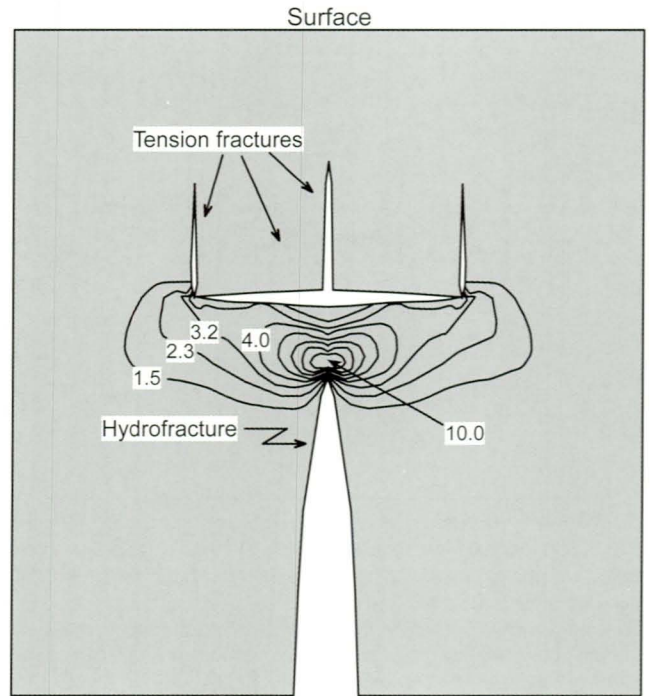

Fig. 10. Same model as in Fig. 9, except that a third joint has been added (in the centre) and the weak contact is here twice as long as in the previous (Fig. 9) model.

ratio of 0.25 is used and, for the first two models (Figs. 9-10), also a uniform Young's modulus of 10 GPa. In the third and fourth models (Figs. 11-12), however, there is a softer layer of 5 GPa embedded in the stiffer layer of 10 GPa, representing layering within the gneiss (Figs. 1-3). As before, the joints and horizontal contacts in the rock are modelled as internal springs with a stiffness of 6 MPa/m. Here, this stiffness may be taken as representative of a soft, but elastic, infill in a joint and a weak sedimentary or soil material at a contact. For comparison, small-scale laboratory samples of clay and weak mudstone have Young's moduli so low as 3 MPa (Bell 2000). Nearly identical results were obtained in model runs where the contacts and joints were open (empty) and thus with zero material stiffness.

In the first model (Fig. 9), a hydrofracture tip at a depth of 0.5 units below the surface approaches three discontinuities, presented by two vertical joints and a horizontal contact, each with a length of 0.2 units. This model reflects, for example, the mechanical effects of a vertical hydrofracture approaching the surface in Fig. 4. All the three discontinuities open up, and tensile stresses concentrate around the tips of the contact and the lower tips of the joints. These stress concentrations indicate a tendency for the joints and the contact to link up, as is seen in the next model (Fig. 10), where a new central joint has also been added. The contact has the greatest opening, followed by that of the central joint (Fig. 10) and, then, the joints to each side. All joints have the greatest openings in their deeper parts.

The next two models (Figs. 11-12) show the effects of mechanical layering on discontinuities opening ahead of a propagating hydrofracture. A soft layer B, with a Young's

modulus of 5 GPa, is embedded in a layer A of 10 GPa, both of which have a Poisson's ratio of 0.25. There are two vertical discontinuities, each of length 0.4 units and presented by internal springs of stiffness 6 MPa/m that reach the surface. Fig. 11 shows that, even if the difference in stiffness between
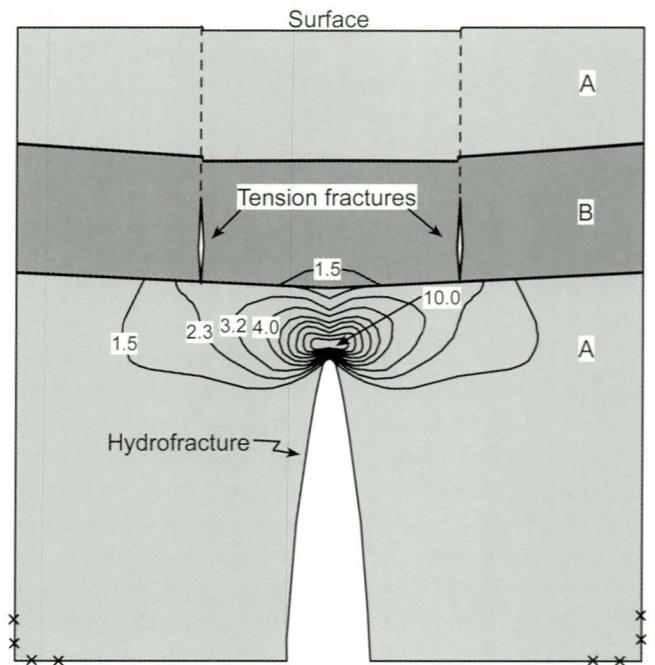

Fig. 11. Boundary-element model showing how the tensile stress, in mega-pascals, around the tip of a vertical hydrofracture opens up vertical joints into tension fractures. The joints are located in a soft layer B (Young's modulus 5 GPa) embedded in a stiffer layer A (Young's modulus 10 GPa). The soft layer reduces the tensile stresses associated with the hydrofracture tip.
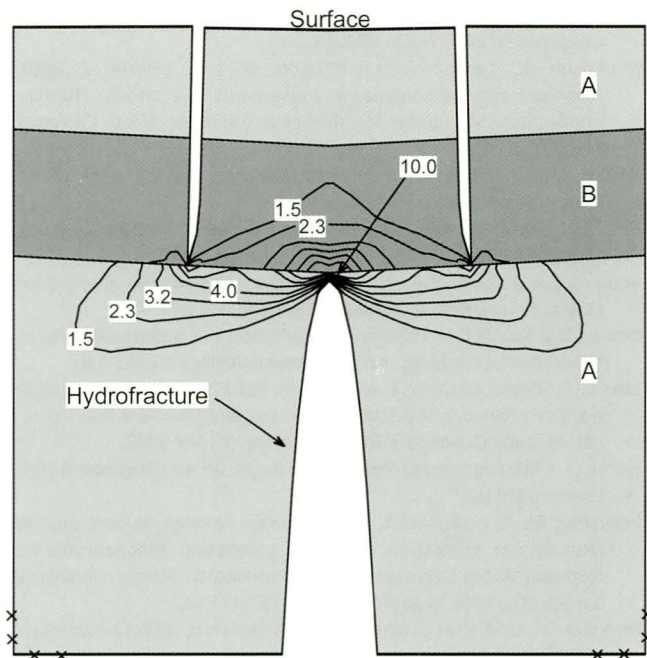
Fig. 12. Same model as in Fig. 11 except that the tip of the hydrofracture here meets with the bottom of the soft layer B.

layers A and B is only by a factor of 2, the tensile stress related to the hydrofracture is much diminished in the soft layer. There is a small opening of the vertical joints in their deepest parts while the near-surface parts remain closed.

When, however, the hydrofracture has propagated an additional 0.1 unit towards the surface, that is, to the bottom of the soft layer B, there is considerable opening of the joints, the maximum being at the free surface (Fig. 12). Thus, for the given loading conditions, when the hydrofracture is at 0.4 units below the free surface, the geometry of the vertical discontinuities changes from the maximum opening being in their deepest parts to its being at the surface. The aperture of an extension fracture commonly becomes much larger at a free surface, or at an open, sliding discontinuity, because of the lack of elastic constraint (Fig. 2).

Stress fields in Norway

The numerical models above consider two loading conditions: external tensile stress and internal fluid overpressure. Here we explore briefly how these loading conditions match with current ideas on the stress field in Norway.

The present-day stress field in Norway has recently been subject to a detailed study, using focal mechanisms, overcoring and borehole breakout data (Fejerskov et al. 2000, Hicks et al. 2000). For West Norway, the main stress is a WNW-ESE-trending compression offshore and a weaker NE-SW-trending extension onshore. The offshore horizontal compression is widely attributed to ridge push (Fejerskov & Lindholm 2000). Both the onshore extension as well as the offshore compression can, however, partly be explained in terms of the inferred glacial erosion and postglacial uplift, depending

on where the margin of the uplifted crustal plate is taken to be (Gudmundsson 1999). Thus, the present-day stress field in Norway depends on its late-glacial history.

There is considerable evidence that the whole of Norway became deglaciated during the period from 8000 to 12,000 B.P. The deglaciation began in the coastal areas (Mangerud 1991, Sejrup et al. 2000) and continued to the highlands where it was essentially complete some 8000 years ago (Mangerud 1991, Nesje & Dahl 2002). In West Norway, the postglacial stress field generated neotectonic activity (Anundsen et al. 2002, Helle et al. 2000). The best documented neotectonic activity in Norway, however, is from the Lapland province in the far north where several reverse and normal faults have been active in the Holocene, some up to the present (Olesen 1992, Dehls et al. 2000), and given rise to hydrological changes (Olesen et al. 2000).

During deglaciation in the coastal areas, temporary tensile stresses may have followed the initial compressive stresses associated with the formation of the horizontal exfoliation fractures (Fig. 1). Because rocks are much weaker in tension than in compression, the linking up of existing joints and fractures subject to suitably oriented tensile stresses (Figs. 7, 8) is much more likely than for an equally large compressive stress. Extension is still occurring in some coastal parts of West Norway (Hicks et al. 2000). Postglacial tensile stresses at shallow crustal depths are thus likely to have been common, thereby supporting the use of tensile loading in some of the numerical models (Figs. 7, 8).

The other numerical models use internal fluid overpressure as the only loading mechanism (Figs. 9-12). This type of loading emphasises the basic conditions for the propagation of vertical hydrofractures. The models in Figs. 9-12 also indicate that at least some of the horizontal exfoliation fractures (Figs. 1-3) may have opened up during flow of an overpressured groundwater associated with the hydrofracture propagation. Similar suggestions have been made for horizontal fractures in Sweden, some of which are thought to be partly generated by fluid overpressure beneath the retreating ice front during deglaciation (Talbot 1999).

Discussion

The relationship between current postglacial uplift rates and yield of groundwater wells (Rohr-Torp 1994) is of fundamental importance in the bedrock hydrogeology of Norway. To understand this relationship in mechanical terms we must explain how the rate of uplift affects the yield. The most likely physical parameter to be affected by postglacial uplift and associated stresses is the hydraulic conductivity. In the bedrock of Norway, hydraulic conductivity is commonly almost entirely determined by interconnected fractures. How these fractures become interconnected and grow is thus perhaps the key to understanding this empirical relationship.

In this paper we use numerical models to indicate some of the basic ways by which interconnected fracture systems

may develop, using fractures from the coastal areas of Norway as examples (Figs. 1-4). How these fracture systems grow affects their effectiveness in transporting groundwater. For example, when the initially offset fractures link up through transverse shear fractures (Figs. 7, 8) the transverse fractures may limit the groundwater transport of the system. This follows because the normal compressive stress on a shear fracture is greater than the minimum compressive principal stress so that the overpressure of groundwater flowing through a transverse fracture is usually less than that of groundwater flowing through an extension fracture. Also, for a given controlling dimension of a fracture, the aperture of such a transverse fracture is normally less than that of an equal-sized extension fracture. In mineral vein systems in Norway and elsewhere, veins in shear fractures are normally thinner than veins in extension fractures (Gudmundsson et al. 2001).

When the groundwater pathway is formed by propagating hydrofractures (Figs. 9-12), the direction of subsequent groundwater flow along the pathway depends on several parameters. For example, once the hydrofracture reaches the contact in Fig. 10, the groundwater could, theoretically, flow into any of the vertical joints. Although the opening of the central joint is the greatest, and would thus normally favour the groundwater flow, the pressure gradient also influences the flow direction. For hydrofractures in an elastic crust, the pressure gradient depends on the state of stress in the host rock (Gudmundsson et al. 2001, Gudmundsson 2001). By contrast, if the rock behaved in a rigid manner subsequent to the opening of the discontinuities, the eventual flow direction of groundwater would be partly determined by the hydraulic gradient.

In conclusion, the data and models presented in this paper indicate that rapid erosion and postglacial uplift are likely to have generated stress fields suitable for the linking up and growth of interconnected fracture systems in various parts of Norway. In particular, temporary tensile stresses and associated fracture growth may have significantly increased the hydraulic conductivity in the bedrock of Norway. The potential tensile stresses increase with increasing rate of postglacial uplift (Gudmundsson 1999) so that the fracture-generated permeability and associated yield of bedrock groundwater wells would be expected to follow empirical relationships similar to those proposed by Rohr-Torp (1994).

Acknowledgements

References

Acocella, V., Gudmundsson, A. & Funiciello, R. 2000: Interaction and linkage of extension fractures and normal faults: examples from the rift zone of Iceland. *Journal of Structural Geology 22*, 1233-1246.

Amadei, B. & Stephansson, O. 1997: *Rock Stress and its Measurement.* Chapman & Hall, London, 490 pp.

Anundsen, K., Grimstveit, L., Harsson, B.G., & Holsen, J. 2002: Measurements of neotectonic movements in southern Norway: implications for former ice thickness estimates. *Norsk Geologisk Tidskrift* (in press).

BEASY, 1991: *The Boundary Element Analysis System User Guide.* Computational Mechanics, Boston.

Bell, F.G. 2000: *Engineering Properties of Soils and Rocks*, 4th edn. Blackwell, Oxford, 482 pp.

Brebbia, C.A. & Dominguez, J. 1989: *Boundary Elements: an Introduction Course.* Computational Mechanics, Boston, 314 pp.

Cox, S.J.D. & Scholz, C.H. 1988: On the formation and growth of faults: an experimental study. *Journal of Structural Geology 10*, 413-430.

Dehls, J.F., Olesen, O., Olsen, L. & Blikra, L.H. 2000: Neotectonic faulting in northern Norway; the Stuoragurra and Nordmannvikdalen postglacial faults. *Quaternary Science Reviews 19*, 1447-1460.

Farmer, I. 1983: *Engineering Behaviour of Rocks*, 2nd ed. Chapman & Hall, London, 208 pp.

Fejerskov, M. & Lindholm, C. 2000: Crustal stresses in and around Norway: an evaluation of stress generating mechanisms. In: Nøttvedt, A. (ed.), Dynamics of the Norwegian Margin. *Geological Society of London, Special Publication 167*, 451-467.

Fejerskov, M., Lindholm, C., Myrvang, A. & Bungum, H. 2000: Crustal stress in and around Norway: compilation of in-situ stress observations. In: Nøttvedt, A. (ed.), Dynamics of the Norwegian Margin. *Geological Society of London, Special Publication 167*, 441-449.

Fossen H. & Dunlap, W.J. 1999. On the age and tectonic significance of Permo-Triassic dikes in the Bergen-Sunnhordaland region, southwestern Norway. *Norsk Geologisk Tidsskrift 79*, 169-177.

Goodman, R. E. 1989: *Introduction to Rock Mechanics*, 2nd ed. Wiley, New York, 562 pp.

Gudmundsson, A. 1992: Formation and growth of normal faults at the divergent plate boundary in Iceland. *Terra Nova 4*, 464-471.

Gudmundsson, A. 1999: Postglacial crustal doming, stresses and fracture formation with application to Norway. *Tectonophysics 307*, 407-419.

Gudmundsson, A. 2000: Fracture dimensions, displacements and fluid transport. *Journal of Structural Geology 22*, 1221-1231.

Gudmundsson, A. 2001: Fluid overpressure and flow in fault zones: field measurements and models. *Tectonophysics 336*, 183-197.

Gudmundsson. A., Brynjolfsson., S. & Jonsson, M.T. 1993: Structural analysis of a transform fault-rift zone junction in North Iceland. *Tectonophysics 220*, 205-221.

Gudmundsson, A., Berg, S.S., Lyslo, K.B. & Skurtveit, E. 2001: Fracture networks and fluid transport in active fault zones. *Journal of Structural Geology 23*, 343-353.

Hanssen, T.H. 1998. Rock stresses and tectonic activity. In: Fjellsprengingsteknikk, Bergmekanikk/Geoteknikk. Trondheim, Norway, Chapter, 1-24.

Helle, S.K., Rye, N., & Stabell, B. 2000: Shoreline displacement and fault activity in the Hardangerfjord, western Norway, after the deglaciation. Geonytt, Norsk Geologisk Forening 24, Norsk Geologisk Vintermøte, Trondheim 6-9 January.

Hicks, E.C., Bungum, H. & Lindholm, C. 2000: Stress inversion of earthquake focal mechanism solutions from onshore and offshore Norway. *Norsk Geologisk Tidsskrift 80*, 235-250.

Hudson, J.A. & Harrison, J.P. 1997: *Engineering Rock Mechanics: an Introduction to the Principles.* Pergamon, Oxford, 444 pp.

Jaeger, J.C. & Cook, N.G.W. 1979. *Fundamentals of Rock Mechanics*, 3rd ed. Chapman & Hall, London, 593 pp.

Johnson, A.M. 1970: *Physical Processes in Geology.* Freeman, Cooper & Company, San Francisco, 577 pp.

Jumikis, A. R. 1979: *Rock Mechanics.* Trans Tech Publications, Clausthal, 356 pp.

Mangerud, J. 1991: The Scandinavian Ice Sheet through the last interglacial/glacial cycle. In: Frenzel, B. (ed.), Problems in the History of the Climate During the Last 130,000 Years. G. Fisher, Stuttgart, 307-330.

Mansfield, C. & Cartwright, J. 2001: Fault growth by linkage: observations

and implications from analogue models. *Journal of Structural Geology 23*, 745-763

Morland, G. 1997: *Petrology, Lithology, Bedrock Structures, Glaciation and Sea Level. Important Factors for Groundwater Yield and Composition of Norwegian Bedrock Boreholes?* Ph.D. Thesis, Montanuniversitat Leoben, 274 pp.

Mörner, N.A. 1980: The Fennoscandian uplift: geological data and their geodynamic implications. *In*: Mörner, N.A. (ed.), Earth Rheology, Isostacy and Eustacy. Wiley, New York, pp.251-284.

Nesje, A. & Dahl, S.O., 2002. Late glacial and Holocene glaciers and climate in southern Norway. *Encyclopedia of Quaternary Science* (in press).

Olesen, O. 1992: The Stuoragurra Fault, evidence of neotectonics in the Precambrian of Finnmark, northern Norway. *Norsk Geologisk Tidsskrift 68*, 107-118.

Olesen, O., Dehls, J., Hilmo, B.O. & Olsen, L., 2000: Neotectonics and seismic pumping of groundwater and hydrocarbons in Norway. *Geonytt*, Norsk Geologisk Forening 24, Norsk Geologisk Vintermøte, Trondheim 6-9 January.

Rohr-Torp, E. 1994: Present uplift rates and groundwater potential in Norwegian hard rocks. *Norges geologiske undersøkelse Bulletin 426*, 47-52.

Sejrup, H.P., Larsen, E., Landvik, J., King, E.L., Haflidason, H. & Nesje, A., 2000: Quaternary glaciations in sourthern Fennoscandia; evidence from south-western Norway and the northern North Sea region. *Quaternary Science Reviews 19*, 667-685.

Singhal, B.B.S. & Gupta, R.P. 1999: *Applied Hydrogeology of Fractured Rocks*. Kluwer, London, 400 pp.

Stauffer, D. & Aharony, A. 1994: *Introduction to Percolation Theory*, 2nd ed. Taylor & Francis, London, 181 pp.

Sundvoll, B. & Larsen, B.T. 1993: Rb-Sr and Sm-Nd relationships in dyke and sill intrusions in the Oslo Rift and related areas. *Norges geologiske undersøkelse Bulletin 425*, 25-42.

Talbot, C. J. 1999: Ice ages and nuclear waste isolation. *Engineering Geology 52*, 177-192.

Thon, A., 1985: The Gullfjellet Ophiolite Complex and the structural evolution of the Major Bergen Arc, West Norwegian Caledonides. *In*: Gee, D. G. & Sturt, B. A. (eds.), *The Caledonide Orogen – Scandinavia and Related Areas, part 1*. John Wiley & Sons, Chichester, 671–677.

Torsvik, T.H., Andersen, T.B., Eide, E.A. & Walderhaug, H.J. 1997: The age and tectonic significance of dolerite dykes in western Norway. *Journal of the Geological Society, London 154*, 961-973.